Title: Modelling biome-scale root reinforcement and slope stability

Author: Hales, T.C.*

Affiliation: School of Earth and Ocean Sciences, Cardiff University, Cardiff, U.K.

*halest@cf.ac.uk

Running title: Biome driven root reinforcement change

Abstract:

Rapid changes in the composition of hillslope vegetation due to a combination of changing climate and land use make estimating slope stability a significant challenge. The dynamics of root growth on any individual hillslope result in a wide range of root distributions and strengths that are reflected as up to an order of magnitude variability in root cohesion. Hence the challenge of predicting the magnitude of root reinforcement for hillslopes requires both an understanding of the magnitude and variability of root distributions and material properties (e.g. tensile strength, elasticity). Here I develop a model for estimating the reinforcement provided by plant roots based on the distribution of biomass measured at the biome level and a compilation of root tensile strength measurements measured across a range of vegetation types. The model modifies the Wu/Waldron method of calculating root cohesion to calculate the average lateral root cohesion and its variability with depth using the Monte Carlo method. The model was validated in two ways, the first against the predicted depth-reinforcement characteristics of Appalachian soils and the second using a global dataset of landslides. Model results suggest that the order of magnitude difference in root cohesions measured on individual hillslopes can be captured by the Monte Carlo approach and provide a simple tool to estimate of root reinforcement for data-poor areas. The model also suggests that future hotspots of slope instability will occur in areas where land use and climate convert forest to grassland, rather than changes between different forest structures or forest and shrubland.

Keywords: Root reinforcement, slope stability, vegetation change

Introduction

The spatial distribution of vegetation on Earth is changing rapidly by land use and climate drivers (Crowther et al., 2015, Davies-Barnard et al., 2015, Hansen et al., 2013, Loarie et al., 2009). Vegetation change affects the rates of soil erosion, particularly landsliding, through modification of the reinforcing strength provided by roots (Gabet and Dunne, 2003), and by changing the soil hydrology through interception and increased suction caused by transpiration (Arnone et al., 2016, Band et al., 2012, Keim and Skaugset, 2003). Major changes in the structure of vegetation, such as happens during deforestation (Degraff, 1979, O'loughlin and Ziemer, 1982) or during climate-driven biome shifts (Beckage et al., 2008, Soja et al., 2007) are likely to significantly affect landslide magnitudes and frequencies, yet we lack a modeling framework for predicting this effect (Fig. 1). A large number of studies have focused on deforestation (Abe and Ziemer, 1991, Brown and Krygier, 1971, Degraff, 1979, Eschner and Patric, 1982, Mills et al., 2003, Montgomery et al., 2000, O'loughlin and Watson, 1979, O'loughlin and Ziemer, 1982, Riestenberg and Sovonick-Dunford, 1983, Sakals and Sidle, 2004, Schmidt et al., 2001, Sidle, 1992, Sidle et al., 2006, Watson et al., 1999, Watson and O'loughlin, 1990, Ziemer, 1981) and natural variability in plant functional type along slopes, usually brush to grass (Gabet and Dunne, 2002, Rice et al., 1969, Watson and O'loughlin, 1985) or montane forest to grass (Mcguire et al., 2016, Rengers et al., 2016) as drivers of dramatic increases in soil erosion and landslide hazards. Remote sensing methods measure vegetation change across the globe, particularly the change in aboveground biomass (e.g. Achard et al., 2002, Hansen et al., 2013, Soja et al., 2007). However, translating these estimates of vegetation change into landslide susceptibility is not currently possible, in part, because we lack a mechanism to estimate the magnitude of soil reinforcement provided by different vegetation types.

Roots reinforce soil against shear forces by elongating in the direction of shear until either they slip from the soil or are broken in tension (Cohen et al., 2011, Pollen-Bankhead and Simon, 2010, Schwarz et al., 2010). Hence, the magnitude of root reinforcement is controlled by the number of roots crossing a shear plane and their ability to resist shearing, which is a function of the friction between soil and root (Pollen, 2007), the amount that roots within a bundle can elongate (Schwarz et al., 2010), and the strength of the roots in tension (Waldron, 1977). Root reinforcement models estimate the shear force required to initiate landsliding parameterised based on measurements made at a single pit or landslide scar (a full derivation of these methods is discussed by Cohen et al., 2011). They are typically divided into two methods that rely on different physical representations of the root bundles. The Wu/Waldron method calculates root reinforcement as a function of the sum of the tensile force at failure of individual roots crossing a failure plane of known area (Waldron, 1977, Wu et al., 1979). The simplicity of this method is its greatest advantage, yet the assumption that all roots break at once is unrealistic (Pollen and Simon, 2005), and leads to overestimates of root cohesion of up to 3 times (Cohen et al., 2011, Schwarz et al., 2010). The main alternative is the fiber-bundle model, where roots are assumed to act as a bundle of individual fibers that break progressively as a function of the amount of load (e.g. Pollen and Simon, 2005) or displacement applied (e.g. Cohen et al., 2011). Fiber-bundle models improve the Wu/Waldron method by accounting for the progressive failure of the root mass (Cohen et al., 2011, Pollen and Simon, 2005).

The belowground conditions that promote soil reinforcement are extremely variable. Measurements of root properties from pit-based field measurements on a single hillslope vary by an order of magnitude, even when controlling for tree size and distance from the stem (Hales et al., 2009, Hales and Miniat, 2017). Soil reinforcement calculated within industrial forests varies between 3 and 5 times, where trees are planted in monoculture and at the same

time (Genet et al., 2008, Schmidt et al., 2001). The variability reflects changes in the distribution of root biomass and diameter distributions as a function of plant age (Osman and Barakbah, 2011), distance from stem (Roering et al., 2003, Schwarz et al., 2012), and the distributions of nutrients, water, and physical barriers within the soil (Stone and Kalisz, 1991). This is modified by changes in the mechanical properties of roots due to root moisture content and water potential (Boldrin et al., 2017, Hales and Miniat, 2017), root age, and physical defects (Cofie and Koolen, 2001, Hales et al., 2013, Schmidt et al., 2001). The high natural variability leads to a significant epistemic uncertainty that must be accounted for in any root reinforcement model.

The challenges associated with natural variability in root reinforcement and uncertainty in root reinforcement models makes it challenging to translate root reinforcement measurements into slope stability models. Commonly used slope stability models such as SHALSTAB (Montgomery and Dietrich, 1994) and SINMAP (Pack et al., 1998) extrapolate an average or uniform distribution of point measurements to estimate cohesion. Others have used the size, geometry and distribution of different trees within a stand to estimate local minima in root strength (Cislaghi et al., 2017, Roering et al., 2003, Sakals and Sidle, 2004, Temgoua et al., 2017). Alternatively, remotely sensed metrics of vegetation, such as normalized density vegetation index (NDVI) and LiDAR-derived canopy heights, have also been related to root reinforcement (Chiang and Chang, 2011, Hwang et al., 2015). In the simplest application, NDVI was linearly related to root reinforcement based on a locally derived range of reinforcement values between 0 and 50kPa (Chiang and Chang, 2011). Regional root distributions have been modelled based on the assumption of water limitation using an ecohydrologic modeling approach (Lepore et al., 2013, Preti et al., 2010, Tron et al., 2014). This eco-hydrological approach has been used to estimate root reinforcement on slopes by taking eco-hydrologically based estimates of root biomass and converting them to a

root reinforcement by using a topological root branching model (Arnone et al., 2016). LiDAR-derived canopy height information combined with empirically derived allocation ratios and biomass measurements can be used to calculate forest-scale root reinforcements (Hwang et al., 2015).

Here, I develop a model of root reinforcement of slopes, using biome-level distributions of root biomass and root tensile strengths. The purpose of the model is twofold. (1) I look to develop a method for estimating root reinforcement, and its variability, for areas where limited or no data about root properties exists. The goal is to produce a model that can be applied easily and at a regional scale. (2) A model that reasonably quantifies the variability of root reinforcement can then be used to assess biomes that are particularly susceptible to changes in root reinforcement (and landslide potential) due to climate and land use change.

Model development

Here, I calculate root reinforcement based on root biomass distributions (e.g. Schenk and Jackson, 2002) and other published root data such as root tensile strengths (e.g. De Baets et al., 2008, Hales et al., 2009) and wood densities (Chave et al., 2009). The model estimates root reinforcement for a particular biome based on empirical measurements of biomass distributions with depth, root tensile strength, and root density. The resulting output provides an estimate of the additional cohesion provided by roots (including the uncertainty in that measurement) as a function of depth for each biome. I test the model using two independent measures, the first is a dataset of 27 pit-scale calculations of root reinforcement for 15 different tree species calculated using a load-distributed fiber-bundle model (Hales et al., 2009, Hales and Miniat, 2017) and the second is a global database of landslide depths, which I compared to calculations of the minimum critical soil depth derived from modelled root cohesions.

At a global scale, the distribution of root belowground biomass has been measured from all terrestrial biomes based on a compilation of point-based root measurements (Jackson et al., 1996, Schenk and Jackson, 2002) (Fig. 2). For each biome, root biomass (units of M/L^2) is distributed using a logistic dose response curve of the form

$$B_T(D) = \frac{B_T}{\left[1 + \left(\dfrac{D}{b_1}\right)^{b_2}\right]},$$

where $B_T(D)$ is the cumulative proportion of total root biomass at a particular depth (D) in the soil column, β_1 (units of L) and β_2 are a shape parameters that are fitted based on the measured cumulative root distributions (Schenk and Jackson, 2002). The error associated with the estimates of β_1 and β_2 is proportional to the number of measurements included in the analysis.

For each depth increment, dividing biomass per unit surface area by the average root density (ρ_r) gives a measure of the total diameter of roots at a particular soil depth which converts to total root cross sectional area per unit soil depth ($r(D)$),

$$r(D)^2 = \left(\frac{B_T(D)}{2r_r}\right)^2 \rho.$$

This is similar to the approach taken by Preti et al. (2010) for converting biomass to root area ratio.

The force that a root breaks in tension depends linearly on their cross-sectional area (Hales et al., 2013, Hales and Miniat, 2017). Hence the force at which roots from a particular tree species break can be determined from the slope of the regression between force at failure and root cross sectional area. I calculated force at failure by randomly sampling from a database containing tensile strength measurements of 67 species (Table 1). I applied a small number of quality control steps to ensure data consistency. Following Hales et al., (2013), I did not distinguish between field and laboratory methods, but limited samples to small

diameters (<5 mm), datasets with greater than 30 samples, and measurements of root strength rather than extraction force. Results reported as tensile strength were converted to force at failure by dividing by root cross sectional area.

Most tensile strength data in the literature is presented as a plot of root diameter against root tensile strength (force/diameter^2), that suggests that small roots are proportionally stronger than larger ones. Given the autocorrelation associated with this plotting method, I chose to plot a linear relationship between root cross sectional area and force at failure (Hales et al., 2013, Hales and Miniat, 2017). The slope of the regression equation represents the average tensile strength (N/m^2) and with the 95% confidence limits of the regression representing the various measurement and environmental uncertainties. To test for any diameter-driven differences in root tensile strength, I linearly regressed the residuals of the force-area plot against root cross sectional area. There was no significant relationship in the residuals for any of the 67 species that I tested. The range of possible root densities and tensile strengths were calculated for each biome by assigning species to biomes based on the location where the data were collected. For each biome the range of densities and tensile strengths were calculated for the dominant plant functional group (i.e. trees, shrubs, grasses).

Root density information is rare in the literature, so I estimated this parameter using one of two methods. The xylem tissue of woody roots and stem wood are the same, so I used published wood densities from the global wood density database (Chave et al., 2009). This method is supported by the similarity between measured root and wood densities for 3 Appalachian tree species (Hwang et al., 2015). Wood densities varied between 400 and 900 kg/m^3 for global species. For shrubs and grasses, average root density was calculated based on published specific root length data and mean root diameter. These estimates are extremely sensitive to the mean root diameter and are considerably more variable (between 40 and 300 m/g) as a result.

Root reinforcement per unit contour width (C_r) for each biome was calculated using a modified version of the Wu/Waldron method,

$$C_r = r \frac{F}{D_s}$$

where F is the total force at failure of the root mass as averaged across a soil of depth D_s. r is a reduction factor that accounts for the overestimation of root reinforcement by the Wu method. The reduction factor approach is similar to that of Runyan and D'Odorico (2014), with r parameterized based on the difference between the Wu method and shear box and FBM-derived estimates of root reinforcement from the literature (e.g. Cohen et al., 2011, Pollen and Simon, 2005, Schwarz et al., 2010). The reduction in strength (r) estimated by fiber bundle models is 1.6 and 2 times (although can be up to 3 times in species dominated by small roots) (Cohen et al., 2011). I calculated lateral reinforcement by dividing the average root tensile force by the soil column depth as basal reinforcements were extremely sensitive to the chosen basal failure plane thickness.

At the scale of this model there are many possible sources of uncertainty. These include estimating the density of roots, their tensile force at failure, the total biomass and its distribution with depth, and the reduction factor. Root density, tensile strength and FBM reduction were sampled from a uniform distribution. The uniform distribution was chosen for these parameters, as the distribution of root densities, tensile strengths, and FBM reductions that are found within our global dataset do not readily fit any statistical distribution. The uniform distribution represents the most conservative approach to parameterizing these values. Uncertainty in root biomass and its distribution were based on the number of observations in a given biome based on Schenk and Jackson's (2002) method. To account for this uncertainty, I calculated the average root reinforcement for a biome based on a Monte Carlo simulation of 1000 different combinations of these parameters.

Model testing

I tested the model using two independently derived field methods. The first, is a comparison between the modelled depth distributions of lateral root reinforcement against FBM-derived estimates of root reinforcement calculated in the Southern Appalachian Mountains (Hales et al., 2009) (Fig. 3 & 4). The forest here is dominated by mixed hardwood forest characteristic of warm temperate forests allowing comparison of the biome-derived reinforcements against the independent measurements from species within that forest.

The second test of the model compares root reinforcements against a global compilation of landslide datasets (Kim et al., 2015, Milledge et al., 2014, Wooten et al., 2007). I calculated the minimum threshold depth for stability for different biomes by rearranging the Mohr-Coulomb equation. This calculation provides an estimate of the minimum expected depth of failure for a given distribution of root reinforcements. For this calculation, friction angle is a significant unknown, so friction angles were randomly chosen from a uniform distribution (with bounds of 30° and 45°), to encompass typical values of friction angle for colluvial soils (e.g. Hales et al., 2009, Schmidt et al., 2001). The minimum failure depths were compared to the measured depths of landslides from each biome (Fig. 5).

Results and Discussion

To assess the first objective, as to whether the model can provide a reliable method for estimating root reinforcement for data poor areas, I compare model results to those from a fibre-bundle model of root reinforcement (Fig. 3). The model compares well with the data both in terms of the depth distribution and variability in root reinforcement. Both the data and model decrease systematically from peak lateral cohesions in very thin (<30cm) soils. This is because the proportion of roots to soil (the root area ratio, RAR) decreases in deeper soils and lateral cohesion is most strongly controlled by RAR. The difference between the data and model results at very shallow soil depths is because the logistic dose function underestimates the relative proportion of roots at very shallow depths. If trying to model stability of very thin

slopes, then it would be best to use the maximum cohesion value from the model. With the exception of a single example of an extremely extensive root system collected downslope of a sugar maple (*Acer saccharum*) range of modeled root cohesions is the similar to the range of measured root cohesion values. When plotted together, the data of figure 3 demonstrate the range of variability in root cohesion within a single forest patch. The distribution of cohesion values produced by the model reflects the distribution that has been measured in the field (Parker et al., 2016) (Fig. 4). Therefore, the probabilistic approach of the modelling in this paper may be able to adequately represent the real distributions of root cohesion on a hillslope. Hence, there is significant promise in using this model in an applied sense.

One significant element of the model is the wide range of cohesion values calculated for a given biome. The range of values reflects both natural variability in the model input parameters and uncertainty associated with the physics of the model. To ascertain whether the wide range of results in the model represents natural variability or model uncertainty, I performed a sensitivity analysis. In the model, the parameters that are affected by the measured natural variability are associated with biomass distributions, tensile strengths, and root densities, while the reduction factor represents the major uncertainty in the characterization of the model. Modelled values of cohesion are most sensitive to the distributions of root tensile strengths. For example, lateral cohesion values at 1 m depth for a warm temperate forest with tensile strengths that range between 9 MPa and 45 MPa (the global range for this biome) vary between 0.5 kPa and 18 kPa. When tensile strength remains constant at 9 MPa and other parameters are varied through their limits, the range of cohesion values is between 0.5 kPa and 4 kPa. In contrast, the value of root density chosen produces only small differences in the value of cohesion at a particular depth, but it strongly controls the distribution of cohesion with depth. Lower density roots occupy a greater root area that will be disproportionately apportioned to areas of concentrated biomass. Hence areas of

higher biomass, close to the surface, will have proportionately higher root cohesions than those with low root biomass. Finally the shape parameters in the biomass distribution are the least sensitive parameters within the model. Changing the reduction factor has no effect on the shape or distribution of root cohesion, but it does affect the minimum and maximum values calculated in the model (by up to a factor of 3). The sensitivity analysis demonstrates that the parameters that reflect the natural variability occurring on slopes (tensile strength and root density) exert much greater effect on the modelled root cohesions than the parameters associated with model uncertainty (the reduction parameter).

The model can be applied to define the range of root cohesion values for a slope, and is particularly useful for areas with no independent measurement of root reinforcement. Predicting the exact location of a landslide on a hillslope may not be necessary for many applications of landslide models, where instead it is susceptibility of a slope to landslides that is of greatest interest. In this case, hazard may be best estimated using the distribution of potential values of root cohesion. Defining the distribution of root cohesions (for a given depth) for a particular vegetation type, allows slope stability models (such as the one shown in Fig. 5) to define the failure conditions across catchments. The advantages of the root cohesion model presented here is that it has a relatively small number of parameters that are well defined empirically, it accurately reproduces both the depth distribution and variability in cohesion to be expected for a given vegetation type. The distribution of root area has been well established as a key element of any estimate of root reinforcement (Abernethy and Rutherfurd, 2001, Cohen et al., 2011). The results of both the modelling exercise and cohesion data from the Southern Appalachians, show that the variability within a particular biome may reflect close to an order of magnitude uncertainty in the value of cohesion (Fig. 3 & 4). Adequately accounting for the uncertainty in the root area ratio, even relatively close to the base of large trees, remains a significant challenge for deterministic models of root

reinforcement, particularly those interested in determining the location of landslide initiation on a hillslope (e.g. Arnone et al., 2016, Cislaghi et al., 2017, Temgoua et al., 2017). When combined with the challenges of estimating the depth of colluvium on a hillslope (Parker et al., 2016) and with the spatial distribution of soil material properties (Milledge et al., 2014), a more deterministic understanding of landslide initiation requires further work.

The primary role of the additional cohesion provided by tree roots is to modify the depth of the failure plane (Selby, 1993). The proposed root reinforcement model allows us to understand the first order controls that vegetation may play in governing the size and depth distribution of landslides (Fig. 5). At a first order, there are significant differences in the total biomass of warm and cool temperate forests and Mediterranean shrublands and vegetation growing in extreme climates (boreal forests and deserts) and for grasslands in any climate (Fig. 2). As a result, both the minimum predicted failure depth and the measured depth of landslides are deeper than those initiated in grasslands (Fig. 5). The model performs best for cool temperate forests and Mediterreanean shrublands (Fig. 5A & C), where the average of our 10,000 estimates of cohesion generally brackets the lower limit of landslide susceptibility and all apart from 1 landslide fall above the minimum cohesion estimated by the model. Warm temperate forests have a very wide range of depths of landslide initiation and modeled cohesions (Fig 4B). Cohesion estimates for grasslands are the least reliable, primarily because landslides can occur at very low slope angles in these landscapes. Lateral cohesion estimates for grassland slopes are extremely low due to their low biomass and shallow depth distributions. When cohesions approach 0 Pa, the Mohr-Coulomb equation suggests that there is no minimum depth for landslide initiation. It could be possible that cohesions could approach 0 Pa within some grassland settings.

Despite differences in biomass distribution and tensile strength, the biome-level model demonstrates that there is very little difference between forests and Mediterranean

shrublands in terms of the additional cohesion, despite significant differences in the root properties. Where they do differ is in terms of shape of the tail of the root cohesion distribution (Fig. 4). Warm temperate forests, where the strongest roots have been measured, include some of the highest cohesion values and have a more strongly skewed distribution of root strengths. When this is examined against the global dataset of landslide depths, warm temperate forests support some of the thickest shallow landslide deposits (Fig. 5). In the case of Appalachian forests (where much of the warm temperate data has been collected), thicker soils appear to more likely be related to differences in the material properties of the soil, dominantly root cohesion, than to hydrological triggering factors (Parker et al., 2016). The model also defines a wide range of potential soil failure planes for these forests. In contrast, Mediterranean shrublands produce roots that have a smaller range of lower root tensile strengths. While the high biomass in these areas produces a similar mean root cohesion to warm temperate forests, the lack of strong roots in this environment means that high values (>10 kPa) of root cohesion are rare. Landslides in these landscape tend to have lower escarpment heights (Fig. 5)

Another application of this modeling framework is to understand how changes in vegetation may affect slope stability. A number of mechanisms have been proposed to affect the distribution of vegetation on hillslopes. Climate change, particularly the distribution of precipitation and temperature affects the distribution of the vegetation (Beckage et al., 2008), and could potentially result in significant future changes in the vegetation composition of hillslopes (Loarie et al., 2009). Changes in vegetation associated with human activity has provided more rapid and measureable changes to hillslope vegetation over the past century (Hansen et al., 2013). These include tree death associated with the introduction of disease and parasites (Ford et al., 2011) and deforestation (Hansen et al., 2013). The model results suggest that due to the natural variability in forest landscapes, slope stability in mixed forests

is likely to be insensitive to the removal of individual species. However, slope stability in monocultures is likely to be very sensitive to land use change. For example, the model could be used to calculate changes in root reinforcement associated with a climate-driven shift from tundra to boreal forests. The results can be readily coupled with slope stability models to provide an understanding of potential changes in landsliding without a priori knowledge of the rooting strengths and distributions. Hence, this model may provide a useful framework for examining global shifts in landslide frequency due to vegetation change.

Conclusions

I developed a regional scale model for estimating the reinforcement provided by plant roots based on the distribution of biomass measured at the biome level and a compilation of root tensile strength measurements measured across a range of vegetation types. The model demonstrates that much of the variability in the depth distribution of root cohesion within a particular biome reflects the uncertainty in the strength and distribution of plant roots. Uncertainties captured by this Monte Carlo approach reflect an order of magnitude difference in root cohesions measured on individual hillslopes. The cohesion values can be added to a slope stability model that coincide with the minimum depths of failure for global shallow landslides. Finally the data suggest that changes in vegetation structure that dramatically change the depth distribution of roots are likely to affect the size and frequency of landsliding, while more subtle changes, such as those at the species level are likely to have relatively little effect on slope stability.

References:

Abdi E, Majnounian B, Genet M, Rahimi H. 2010. Quantifying the effects of root reinforcement of Persian Ironwood (*Parrotia persica*) on slope stability; a case study: Hillslope of Hyrcanian forests, northern Iran. Ecological Engineering **36**: 1409-1416

Abe K, Ziemer RR. 1991. Effect of tree roots on shallow-seated landslides. In *Proceedings of the IUFRO technical session on geomorphic hazards in managed forests*, Rice RM (ed). General Technical Report PSW-GTR-130: Montreal, Canada.

Abernethy B, Rutherfurd ID. 2001. The distribution and strength of riparian tree roots in relation to riverbank reinforcement. Hydrological Processes **15**: 63-79. DOI: 10.1002/hyp.152

Achard F, Eva HD, Stibig H-J, Mayaux P, Gallego J, Richards T, Malingreau J-P. 2002. Determination of Deforestation Rates of the World's Humid Tropical Forests. Science **297**: 999-1002. DOI: 10.1126/science.1070656

Anderson CJ, Coutts MP, Ritchie RM, Campbell DJ. 1989. Root extraction force measurements for Sitka Spruce. Forestry **62**: 127-137

Arnone E, Caracciolo D, Noto LV, Preti F, Bras RL. 2016. Modeling the hydrological and mechanical effect of roots on shallow landslides. Water Resources Research **52**: 8590-8612. DOI: 10.1002/2015WR018227

Band LE, Hwang T, Hales TC, Vose J, Ford C. 2012. Ecosystem processes at the watershed scale: Mapping and modeling ecohydrological controls of landslides. Geomorphology **137**: 159-167. DOI: 10.1016/j.geomorph.2011.06.025

Beckage B, Osborne B, Gavin DG, Pucko C, Siccama T, Perkins T. 2008. A rapid upward shift of a forest ecotone during 40 years of warming in the Green Mountains of Vermont. Proceedings of the National Academy of Sciences of the United States of America **105**: 4197-4202. DOI: 10.1073/pnas.0708921105

Bischetti GB, Chiaradia E, Epis T, Morlotti E. 2009. Root cohesion of forest species in the Italian Alps. Plant and Soil **324**: 71-89. DOI: 10.1007/s11104-009-9941-0

Bischetti GB, Chiaradia EA, Simonato T, Speziali B, Vitali B, Vullo P, Zocco A. 2005. Root strength and root area ratio of forest species in Lombardy (Northern Italy). Plant and Soil **278**: 11-22

Boldrin D, Leung AK, Bengough AG. 2017. Root biomechanical properties during establishment of woody perennials. Ecological Engineering. DOI: http://dx.doi.org/10.1016/j.ecoleng.2017.05.002

Brown GW, Krygier JT. 1971. Clear-Cut Logging and Sediment Production in the Oregon Coast Range. Water Resources Research **7**: 1189-1198

Burylo M, Hudek C, Rey F. 2011. Soil reinforcement by the roots of six dominant species on eroded mountainous marly slopes (Southern Alps, France). Catena **84**: 70-78. DOI: http://dx.doi.org/10.1016/j.catena.2010.09.007

Burylo M, Rey F, Mathys N, Dutoit T. 2012. Plant root traits affecting the resistance of soils to concentrated flow erosion. Earth Surface Processes and Landforms **37**: 1463-1470. DOI: 10.1002/esp.3248

Chave J, Coomes D, Jansen S, Lewis SL, Swenson NG, Zanne AE. 2009. Towards a worldwide wood economics spectrum. Ecology Letters **12**: 351-366. DOI: 10.1111/j.1461-0248.2009.01285.x

Chiang S-H, Chang K-T. 2011. The potential impact of climate change on typhoon-triggered landslides in Taiwan, 2010–2099. Geomorphology **133**: 143-151. DOI: http://dx.doi.org/10.1016/j.geomorph.2010.12.028

Cislaghi A, Chiaradia EA, Bischetti GB. 2017. Including root reinforcement variability in a probabilistic 3D stability model. Earth Surface Processes and Landforms: n/a-n/a. DOI: 10.1002/esp.4127

Cofie P, Koolen AJ. 2001. Test speed and other factors affecting the measurements of tree root properties used in soil reinforcement models. Soil & Tillage Research **63**: 51-56. DOI: 10.1016/s0167-1987(01)00225-2

Cofie P, Koolen AJ, Perdok UD. 2000. Measurement of stress-strain relationship of beech roots and calculation of the reinforcement effect of tree roots in soil-wheel systems. Soil & Tillage Research **57**: 1-12. DOI: 10.1016/s0167-1987(00)00126-4

Cohen D, Schwarz M, Or D. 2011. An analytical fiber bundle model for pullout mechanics of root bundles. Journal of Geophysical Research **116**: doi:10.1029/2010JF001886

Crowther TW, Glick HB, Covey KR, Bettigole C, Maynard DS, Thomas SM, Smith JR, Hintler G, Duguid MC, Amatulli G, Tuanmu MN, Jetz W, Salas C, Stam C, Piotto D, Tavani R, Green S, Bruce G, Williams SJ, Wiser SK, Huber MO, Hengeveld GM, Nabuurs GJ, Tikhonova E, Borchardt P, Li CF, Powrie LW, Fischer M, Hemp A, Homeier J, Cho P, Vibrans AC, Umunay PM, Piao SL, Rowe CW, Ashton MS, Crane PR, Bradford MA. 2015. Mapping tree density at a global scale. NATURE **advance online publication**. DOI: 10.1038/nature14967

http://www.nature.com/nature/journal/vaop/ncurrent/abs/nature14967.html - supplementary-information

Davies-Barnard T, Valdes PJ, Singarayer JS, Wiltshire AJ, Jones CD. 2015. Quantifying the relative importance of land cover change from climate and land use in the representative concentration pathways. Global Biogeochemical Cycles **29**: 2014GB004949. DOI: 10.1002/2014GB004949

De Baets S, Poesen J, Reubens B, Wemans K, De Baerdemaeker J, Muys B. 2008. Root tensile strength and root distribution of typical Mediterranean plant species and their contribution to soil shear strength. Plant and Soil **305**: 207-226

DeGraff JV. 1979. Initiation of shallow mass movement by vegetative-type conversion. Geology **7**: 426-429. DOI: 10.1130/0091-7613(1979)7<426:iosmmb>2.0.co;2

Eschner AR, Patric JH. 1982. Debris avalanches in Eastern upland forests. Journal of Forestry **80**: 343-347

Fan C-C, Chen Y-W. 2010. The effect of root architecture on the shearing resistance of root-permeated soils. Ecological Engineering **36**: 813-826

Ford CR, Elliott KJ, Clinton BD, Kloeppel BD, Vose JM. 2011. Forest dynamics following eastern hemlock mortality in the southern Appalachians. Oikos: Doi: 10.1111/j.1600-0706.2011.19622.x

Gabet EJ, Dunne T. 2002. Landslides on coastal sage-scrub and grassland hillslopes in a severe El Niño winter: The effects of vegetation conversion on sediment delivery. Geological Society of America Bulletin **114**: 983-990. DOI: 10.1130/0016-7606(2002)114<0983:locssa>2.0.co;2

Gabet EJ, Dunne T. 2003. A stochastic sediment delivery model for a steep Mediterranean landscape. Water Resources Research **39**: doi:10.1029/2003WR002341

Genet M, Kokutse N, Stokes A, Fourcaud T, Cai XH, Ji JN, Mickovski S. 2008. Root reinforcement in plantations of *Cryptomeria japonica D. Don*: effect of tree age and stand structure on slope stability. Forest Ecology and Management **256**: 1517-1526. DOI: 10.1016/j.foreco.2008.05.050

Genet M, Li M, Luo T, Fourcaud T, Clément-Vidal A, Stokes A. 2011. Linking carbon supply to root cell-wall chemistry and mechanics at high altitudes in *Abies georgei*. Annals of Botany **107**: 311-320

Genet M, Stokes A, Salin F, Mickovski SB, Fourcaud T, Dumail J-F, van Beek R. 2005. The influence of cellulose content on tensile strength of tree roots. Plant and Soil **278**: 1-9

Hales TC, Cole-Hawthorne C, Lovell L, Evans S. 2013. Assessing the accuracy of simple field based root strength measurements. Plant and Soil **372**: 553-565. DOI: 10.1007/s11104-013-1765-2

Hales TC, Ford CR, Hwang T, Vose JM, Band LE. 2009. Topographic and ecologic controls on root reinforcement. Journal of Geophysical Research **114**: doi:10.1029/2008JF001168

Hales TC, Miniat CF. 2015. Hillslope-scale root cohesion driven by soil moisture conditions. Earth Surface Processes and Landforms: in review

Hales TC, Miniat CF. 2017. Soil moisture causes dynamic adjustments to root reinforcement that reduce slope stability. Earth Surface Processes and Landforms **42**: 803-813. DOI: 10.1002/esp.4039

Hansen MC, Potapov PV, Moore R, Hancher M, Turubanova SA, Tyukavina A, Thau D, Stehman SV, Goetz SJ, Loveland TR, Kommareddy A, Egorov A, Chini L, Justice CO, Townshend JRG. 2013. High-Resolution Global Maps of 21st-Century Forest Cover Change. Science **342**: 850-853. DOI: 10.1126/science.1244693

Hwang T, Band LE, Hales TC, Miniat CF, Vose JM, Bolstad PV, Miles B, Price K. 2015. Simulating vegetation controls on hurricane-induced shallow landslides with a distributed ecohydrological model. Journal of Geophysical Research: Biogeosciences: 2014JG002824. DOI: 10.1002/2014JG002824

Jackson RB, Canadell J, Ehleringer JR, Mooney HA, Sala OE, Schulze ED. 1996. A global analysis of root distributions for terrestrial biomes. Oecologia **108**: 389-411

Ji J, Kokutse N, Genet M, Fourcaud T, Zhang Z. 2012. Effect of spatial variation of tree root characteristics on slope stability. A case study on Black Locust (*Robinia pseudoacacia*) and Arborvitae (*Platycladus oreintalis*) stands on the Loess Plateau, China. Catena **92**: 139-154

Keim RF, Skaugset AR. 2003. Modelling effects of forest canopies on slope stability. Hydrological Processes **17**: 1457-1467

Kim MS, Onda Y, Kim JK. 2015. Improvement of shallow landslide prediction accuracy using soil parameterisation for a granite area in South Korea. Nat. Hazards Earth Syst. Sci. Discuss. **3**: 227-267. DOI: 10.5194/nhessd-3-227-2015

Lepore C, Arnone E, Noto LV, Sivandran G, Bras RL. 2013. Physically based modeling of rainfall-triggered landslides: a case study in the Luquillo forest, Puerto Rico. Hydrol. Earth Syst. Sci. **17**: 3371-3387. DOI: 10.5194/hess-17-3371-2013

Loades KW, Bengough Ag, Bransby MF, Hallett PD. 2010. Planting density influence on fibrous root reinforcement of soils. Ecological Engineering **36**: 276-284

Loarie SR, Duffy PB, Hamilton H, Asner GP, Field CB, Ackerly DD. 2009. The velocity of climate change. NATURE **462**: 1052-1055

Makarova OV, Cofie P, Koolen AJ. 1998. Axial stress-strain relationships of fine roots of Beech and Larch in loading to failure and in cyclic loading. Soil & Tillage Research **45**: 175-187. DOI: 10.1016/s0933-3630(97)00017-2

Mattia C, Bischetti GB, Gentile F. 2005. Biotechnical characteristics of root systems of typical Mediterranean species. Plant and Soil **278**: doi:10.1007/s11104-005-7930-5

McGuire LA, Rengers FK, Kean JW, Coe JA, Mirus BB, Baum RL, Godt JW. 2016. Elucidating the role of vegetation in the initiation of rainfall-induced shallow landslides: Insights from an extreme rainfall event in the Colorado Front Range. Geophysical Research Letters: 2016GL070741. DOI: 10.1002/2016GL070741

Milledge DG, Bellugi D, McKean JA, Densmore AL, Dietrich WE. 2014. A multidimensional stability model for predicting shallow landslide size and shape across landscapes. Journal of Geophysical Research: Earth Surface **119**: 2014JF003135. DOI: 10.1002/2014JF003135

Mills K, Paul J, Hinkle J, Skaugset AR. 2003. Forest Practices and Mitigation of Debris-Flow Risk in Oregon, USA. In *Debris-Flow Hazards Mitigation: Mechanics, Prediction, and Assessment*, Rickenmann D, Chen CL (eds). Millpress: Rotterdam; 1197-1207.

Montgomery DR, Dietrich WE. 1994. A physically based model for the topographic control on shallow landsliding. Water Resources Research **30**: 1153-1171

Montgomery DR, Schmidt KM, Greenberg HM, Dietrich WE. 2000. Forest clearing and regional landsliding. Geology **28**: 311-314. DOI: 10.1130/0091-7613(2000)28<311:fcarl>2.0.co;2

Norris JE. 2005. Root Reinforcement by Hawthorn and Oak Roots on a Highway Cut-Slope in Southern England. Plant and Soil **278**: doi:10.1007/s11104-005-1301-0

O'Loughlin C, Watson AJ. 1979. Root wood strength deterioration in *Pinus radiata* after clearfelling. New Zealand Journal of Forestry Science **9**: 284-293

O'Loughlin C, Ziemer RR. 1982. The importance of root strength and deterioration rates upon edaphic stability in steepland forests. In *Carbon Uptake and Allocation in Subalpine Ecosystems as a Key to Management*: Proceedings of an IUFRO Workshop; 70-77.

Osman N, Barakbah SS. 2011. The effect of plant succession on slope stability. Ecological Engineering **37**: 139-147

Pack RT, Tarboton DG, Goodwin CN. 1998. The SINMAP Approach to Terrain Stability Mapping. In *8th Congress of the International Association of Engineering Geology*: Vancouver, British Columbia.

Parker RN, Hales TC, Mudd SM, Grieve SDG, Constantine J. 2016. Colluvium supply in humid regions limits the frequency of storm-triggered landslides. Scientific Reports:

Pollen N. 2007. Temporal and spatial variability in root reinforcement of streambanks: Accounting for soil shear strength and moisture. Catena **69**: 197-205

Pollen N, Simon A. 2005. Estimating the mechanical effects of riparian vegetation on stream bank stability using a fiber bundle model. Water Resources Research **41**: doi:10.1029/2004WR003801

Pollen-Bankhead N, Simon A. 2010. Hydrologic and hydraulic effects of riparian root networks on streambank stability: Is mechanical root-reinforcement the whole story? Geomorphology **116**: 353-362

Preti F, Dani A, Laio F. 2010. Root profile assessment by means of hydrological, pedological and above-ground vegetation information for bio-engineering purposes. Ecological Engineering **36**: 305-316. DOI: http://dx.doi.org/10.1016/j.ecoleng.2009.07.010

Preti F, Giadrossich F. 2009. Root reinforcement and slope bioengineering stabilization by Spanish Broom (Spartium junceum L.). Hydrology and Earth System Sciences **13**: 1713-1726

Rengers FK, McGuire LA, Coe JA, Kean JW, Baum RL, Staley DM, Godt JW. 2016. The influence of vegetation on debris-flow initiation during extreme rainfall in the northern Colorado Front Range. Geology. DOI: 10.1130/g38096.1

Rice RM, Crobett ES, Bailey RG. 1969. Soil Slips Related to Vegetation, Topography, and Soil in Southern California. Water Resources Research **5**: 647-659. DOI: 10.1029/WR005i003p00647

Riestenberg MM. 1994. Anchoring of thin colluvium by roots of sugar maple and white ash on hillslopes in Cincinnati. United States Geological Survey Bulletin **2059-E**: 1–25

Riestenberg MM, Sovonick-Dunford S. 1983. The role of woody vegetation in stabilizing slopes in the Cincinatti area, Ohio. Geological Society of America Bulletin **15**: 3-45

Roering JJ, Schmidt KM, Stock JD, Dietrich WE, Montgomery DR. 2003. Shallow landsliding, root reinforcement, and the spatial distribution of trees in the Oregon Coast Range. Canadian Geotechnical Journal **40**: 237-253

Runyan CW, D'Odorico P. 2014. Bistable dynamics between forest removal and landslide occurrence. Water Resources Research **50**: 1112-1130. DOI: 10.1002/2013WR014819

Sakals ME, Sidle RC. 2004. A spatial and temporal model of root cohesion in forest soils. Canadian Journal of Forest Research **34**: 950-958

Schenk HJ, Jackson RB. 2002. The global biogeography of roots. Ecological Monographs **72**: 311-328

Schmidt K, Roering JJ, Stock JD, Dietrich WE, Montgomery DR, Schaub T. 2001. The variability of root cohesion as an influence on shallow landslide susceptibility in the Oregon Coast Range. Canadian Geotechnical Journal **38**: 995-1024

Schwarz M, Cohen D, Or D. 2010. Root-soil mechanical interactions during pullout and failure of root bundles. Journal of Geophysical Research **115**: doi:10.1029/2009JF001603

Schwarz M, Cohen D, Or D. 2012. Spatial characterization of root reinforcement at stand scale: Thoery and case study. Geomorphology **171-172**: 190-200

Selby MJ. 1993. Hillslope materials and processes. Oxford University Press: Oxford

Sidle RC. 1992. A theoretical model of the effects of timber harvesting on slope stability. Water Resources Research **28**: 1897-1910. DOI: 10.1029/92WR00804

Sidle RC, Ziegler AD, Negishi JN, Nik AR, Siew R, Turkelboom F. 2006. Erosion processes in steep terrain-Truths, myths, and uncertainties related to forest management in Southeast Asia. Forest Ecology and Management **224**: 199-225

Soja AJ, Tchebakova NM, French NHF, Flannigan MD, Shugart HH, Stocks BJ, Sukhinin AI, Parfenova EI, Chapin III FS, Stackhouse Jr. PW. 2007. Climate-induced boreal forest change: Predictions versus current observations. Global and Planetary Change **56**: 274-296

Stone EL, Kalisz PJ. 1991. On the maximum extent of tree roots. Forest Ecology and Management **46**: 59-102

Temgoua AGT, Kokutse NK, Kavazović Z, Richard M. 2017. A 3D model applied to analyze the mechanical stability of real-world forested hillslopes prone to landslides. Ecological Engineering **106**: 609-619. DOI: http://dx.doi.org/10.1016/j.ecoleng.2017.06.043

Tosi M. 2007. Root tensile strength relationships and their slope stability implications of three shrub species in the Northern Apennines (Italy). Geomorphology **87**: 268-283. DOI: 10.1016/j.geomorph.2006.09.019

Tron S, Dani A, Laio F, Preti F, Ridolfi L. 2014. Mean root depth estimation at landslide slopes. Ecological Engineering **69**: 118-125. DOI: http://dx.doi.org/10.1016/j.ecoleng.2014.03.019

Waldron LJ. 1977. The shear resistance of root-permeated homogeneous and stratified soil. Journal of the Soil Science Society of America **41**: 843-849

Watson A, Phillips C, Marden M. 1999. Root strength, growth, and rates of decay: root reinforcement changes of two tree species and their contribution to slope stability. Plant and Soil **217**: 39-47

Watson AJ, O'Loughlin C. 1985. Morphology, Strength, and Biomass of Manuka Roots and their Influence on Slope Stability. New Zealand Journal of Forestry Science **15**: 337-348

Watson AJ, O'Loughlin C. 1990. Structural Root Morphology and Biomass of Three Age-Classes of *Pinus Radiata*. New Zealand Journal of Forestry Science **20**: 97-110

Wooten RM, Latham RS, Witt AC, Gillon KA, Douglas TJ, Fuemmeler SJ, Bauer JB, Reid JC. 2007. Landslide hazards and landslide hazard mapping in North Carolina. In *1st North American Landslide Conference*, Schaefer VR, Schuster RL, Turner AK (eds). Association of Environmental and Engineering Geologists: Vail, Colorado; 458-471.

Wu TH, McKinnell III WP, Swanston DN. 1979. Strength of tree roots and landslides on Prince of Wales Island, Alaska. Canadian Geotechnical Journal **16**: 19-34

Zhang C, Chen L, Jiang J. 2014. Why fine tree roots are stronger than thicker roots: The role of cellulose and lignin in relation to slope stability. Geomorphology **206**: 196-202

Zhang C, Chen L, Jiang J, Zhou S. 2012. Effects of gauge length and strain rate on the tensile strength of tree roots. Trees **26**: 1577-1584

Ziemer RR. 1981. Roots and the Stability of Forested Slopes. In *Proceedings of the International Symposium on Erosion and Sediment Transport in Pacific Rim Steeplands*, Davies TRH, Pearce AJ (eds). New Zealand International Association of Hydrolgical Sciences: Christchurch; 343-361.
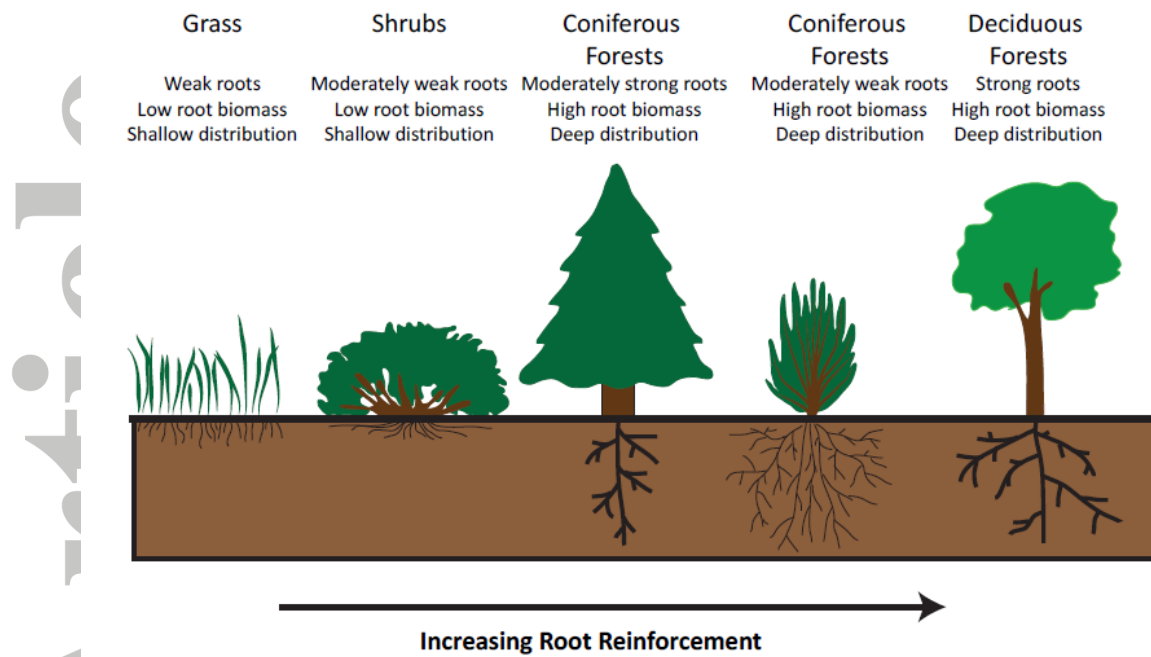
Figure 1: Cartoon depicting how root reinforcement varies as a function of different vegetation types. Trees and Mediterranean shrubs produce the highest root reinforcements due to their extensive subsurface biomass distributions and strong woody roots. Weaker and shallowly rooted vegetation types produce lower root reinforcements
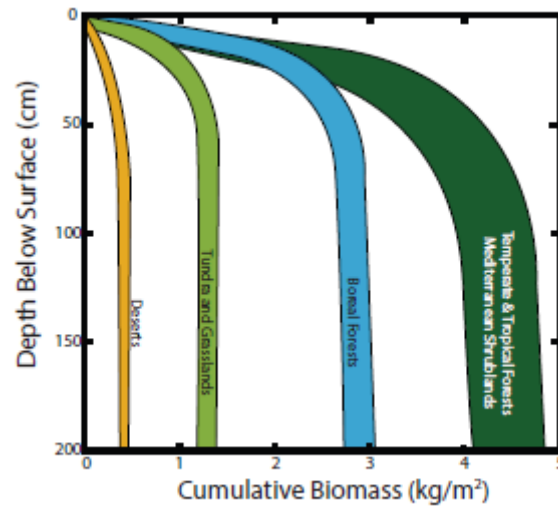
Figure 2: Root biomass distributions for different biomes as estimated by Schenk and Jackson (2002). Plot of cumulative biomass as a function of depth below the soil surface, showing the difference in both the total biomass and its location within the soil column for all major biomes. Forests and Mediterranean shrublands have the highest belowground biomass that is distributed deep within the soil column. Boreal forests are the exception and have roots that do not penetrate as deeply into frozen ground. Tundra and grasslands have small biomasses that are very shallowly distributed, whereas deserts have relatively few roots, but they can be deeply distributed.
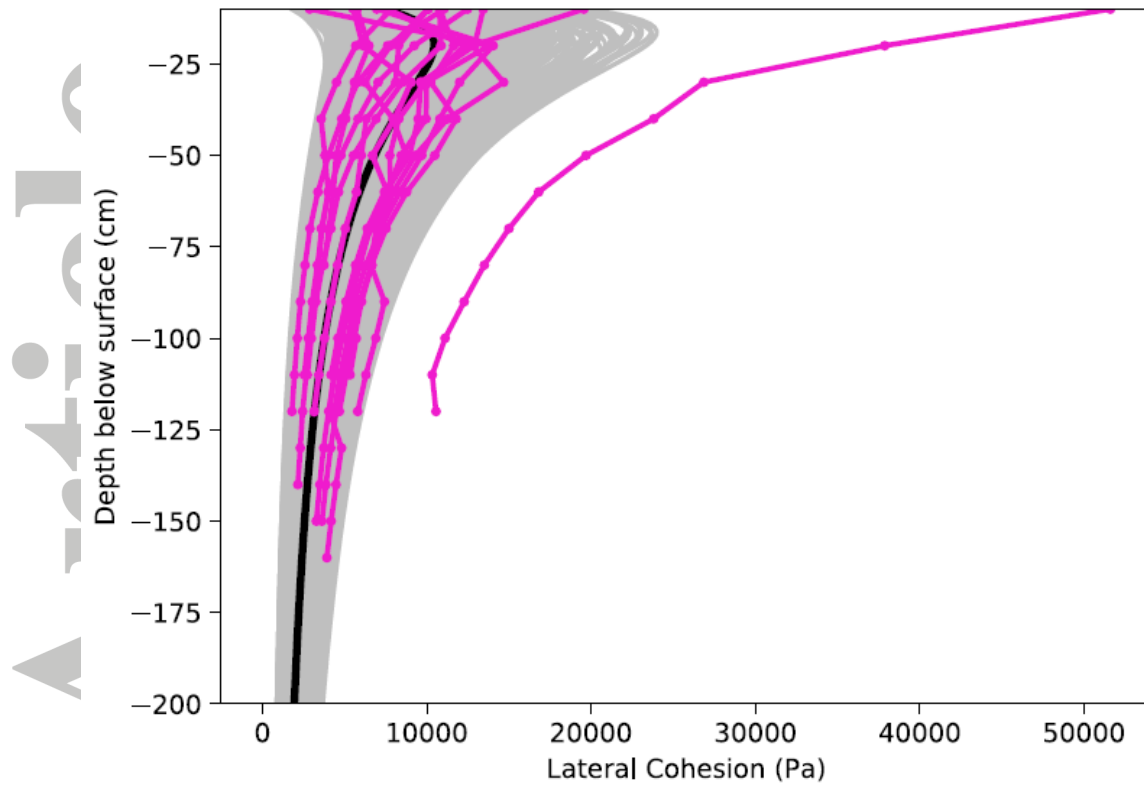
Figure 3: Modelled root reinforcement for a broadleaf temperate forest compared to load-distributed fiber bundle model measurements of root reinforcement (purple lines).

Figure 4. Histograms displaying the distributions of root cohesion for different biomes. (A) The distribution of root cohesions measured in Appalachian soil pits by Hales et al., 2009 and Hales & Miniat, 2017. These can be directly compared to model results for (B) warm temperate forests and contrasted with (C) grasslands and (D) Mediterranean shrublands.
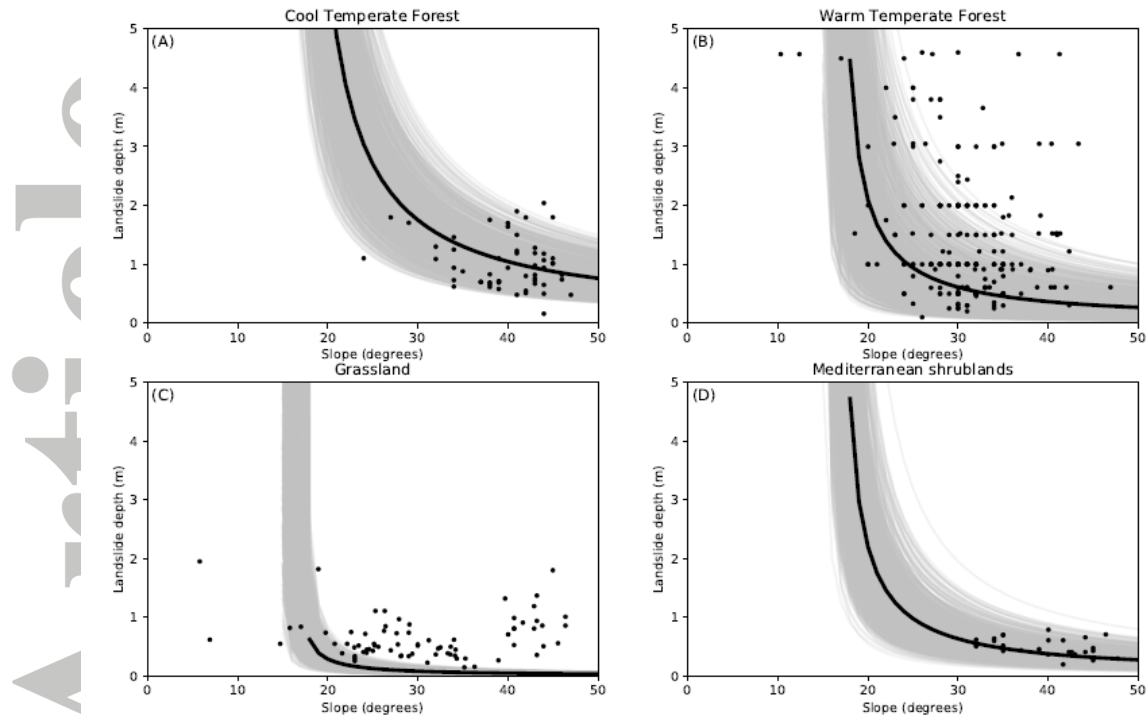
Figure 5: Plots showing the distribution of modeled landslide depths for a range of predicted root cohesions. Black dots represent the depths of landslides from a global compilation. These plots show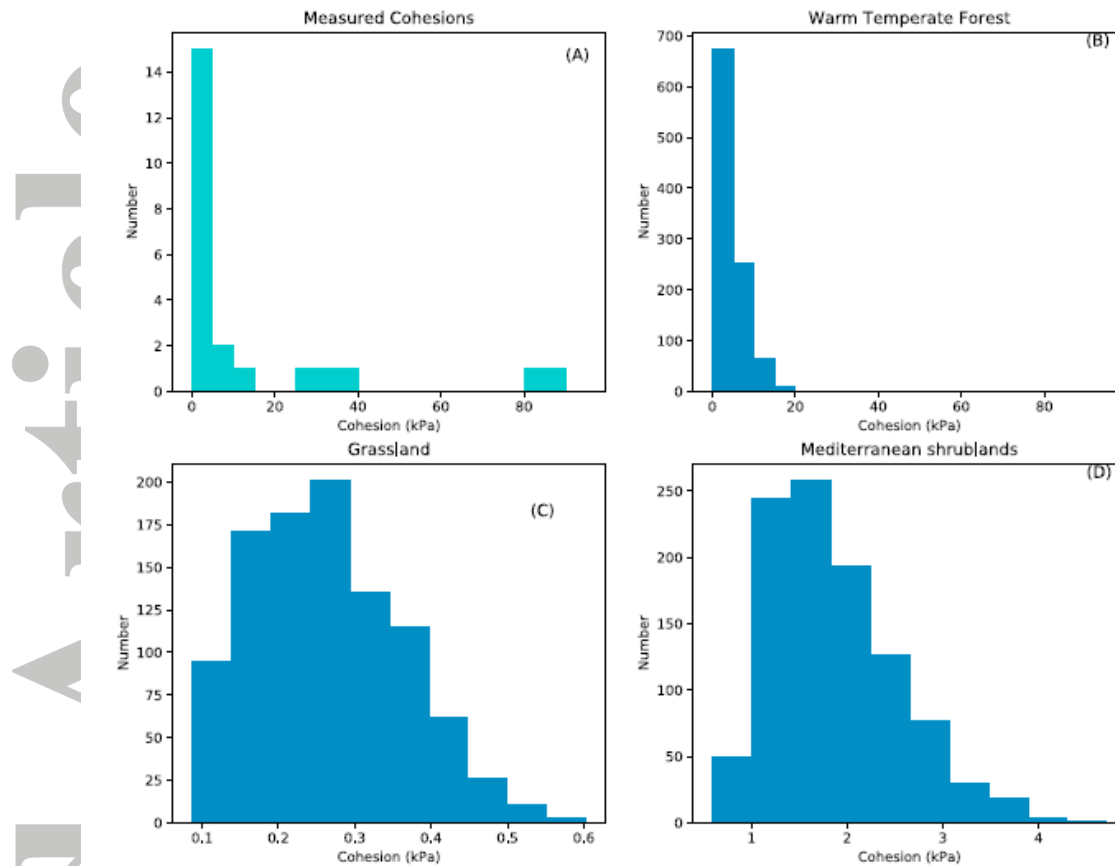 that the modeled root cohesions provide a minimum estimate of root cohesion for these landscapes. The model performs best in forested and shrubland areas, where most landslide fall within the error envelope predicted by the model. The model is less reliable in grassland settings, likely because the very low cohesions may mean that grasslands behave more like cohesionless landscapes and have no obvious minimum failure depth.

Table 1. Table showing the database of biomes, species, densities (derived from Chave et al., 2009), and number of observations. The densities of two grass and shrub species were estimated from specific root length data in the literature, they are likely to be significantly more uncertain than the other density data. * is derived from specific root lengths of Løes & Gahoonia (2004) with mean diameters of Loades et al (2010). § is derived 40-120 m/g SRL and an average root diameter of 0.35mm from Li et al (2017)

Biome	Name	Source	Density	n	Tensile Strength (MPa)	Uncertainty (Mpa)
Boreal	*Abies georgei*	Genet 2011	433	213	14.4	1.1
	Picea abies	Genet 2005	370	27	20.30	3.06
	Picea sitchensis	Hales 2013, Anderson 1989	366	146	9.38	0.47
Cool Temperate Forest	*Acer circinatum*	Schmidt 2001	440	21	27.69	4.18
	Acer macrophyllum	Schmidt 2001	440	13	n/a	n/a
	Acer saccharum	Hales 2009, Rietenberg 1994	440	83	32.04	2.47
	Alnus rubra	Schmidt 2001	370	17	n/a	n/a
	Anaphalis sp	Schmidt 2001	n/a	8	n/a	n/a
	Betula lenta	Hales 2015, Hales 2009	600	419	15.49	2.47
	Betula platyphylla	Zhang 2012	518	38	24.11	1.29
	Castanea sativa	Bischetti 2009, Genet 2005	463	106	15.46	1.02
	Cryptomeria japonica	Genet 2008	400	178	17.42	1.09
	Crataegus monogyna	Norris 2005	n/a	40	n/a	n/a
	Digitalis species	Schmidt 2001	n/a	30	9.61	1.21
	Fagus sylvatica	Bischetti 2005, Cofie 2000, Genet 2005, Makarova 1998	585	270	12.81	1.18
	Larix principis-rupprechtii	Zhang 2012	560	37	11.39	1.14
	Mahonia nervosa	Schmidt 2001	n/a	11	n/a	n/a
	Nephrolepis sp	Schmidt 2001	n/a	8	n/a	n/a
	Parrotia persica	Abdi et al 2010	870	97	22.12	1.78

	Species	Reference				
	Pinus tabulaeformis	Zhang 2014,2012	360	315	14.23	0.36
	Psuedotsuga menziesii	Schmidt 2001	428	126	10.03	0.93
	Quercus mongolicus	Zhang 2012	636	28	20.89	1.33
	Quercus robor	Norris 2005	575	9	n/a	n/a
	Quercus rubra	Hales 2009	560	337	18.72	0.91
	Rubus armeniacus	Schmidt 2001	350	19	n/a	n/a
	Rubus parviflorus	Schmidt 2001	350	18	n/a	n/a
	Sambucus cerulea	Schmidt 2001	460	21	18.69	4.44
	Tsuga heterophylla	Schmidt 2001	420	25	8.18	1.87
	Ulmus pumila	Zhang 2012	544	24	n/a	n/a
Mediterannean Shrubland	*Achnatherum calamagrostis*	Burlyo 2011,2012	n/a	52	n/a	n/a
	Anthyllis cytisoides	deBaets 2008	n/a	54	8.46	1.06
	Aphyllantes monspeliensis	Burlyo 2011	n/a	17	n/a	n/a
	Artemisia barrelieri	deBaets 2008	n/a	32	n/a	n/a
	Atriplex halimus	Mattia 2005, deBaets 2008	n/a	93	27.38	3.94
	Avenula bromoides	deBaets 2008	n/a	52	40.13	4.75
	Brachypodium retusum	deBaets 2008	n/a	33	30.52	5.04
	Dittrichia viscosa	deBaets 2008, Tosi 2007	n/a	113	2.81	0.87
	Dorycnium pentaphyllum	deBaets 2008	n/a	48	11.13	0.98
	Fumana thymifolia	deBaets 2008	n/a	52	11.78	1.53
	Genista cinerea	Burlyo 2011	n/a	29	48.91	4.57
	Helictotrichon filifolium	deBaets 2008	n/a	53	17.51	2.93
	Juncus acutus	deBaets 2008	n/a	45	19.42	3.99
	Limonium supinum	deBaets 2008	n/a	29	9.77	3.25
	Lygeum spartum	Mattia 2005, deBaets 2008	n/a	75	14.83	3.12

	Nerium oleander	deBaets 2008	600	30	5.62	0.96
	Ononis tridentata	deBaets 2008	n/a	46	8.74	0.81
	Ostrya carpinifolia	Bischetti et al 2009	653	38	15.37	1.64
	Phragmites australis	deBaets 2008	866*	20	n/a	n/a
	Pistacia lentiscus	Mattia 2005	700	17	n/a	n/a
	Piptatherum miliaceum	deBaets 2008	n/a	47	76.56	10.89
	Pinus nigra	Burlyo 2011,2012, Genet 2005	417	54	13.45	1.37
	Pinus pinaster	Genet 2005	412	30	15.09	3.37
	Plantago albicans	deBaets 2008	n/a	50	8.10	2.51
	Quercus pubescens	Burlyo 2011	800	9	n/a	n/a
	Retama sphaerocarpa	deBaets 2008	n/a	28	13.72	1.53
	Rosa canina	Tosi 2007	n/a	34	1.48	0.20
	Rosmarinus officinalis	deBaets 2008	n/a	55	8.01	1.11
	Salsola genistoides	deBaets 2008	n/a	26	12.83	3.62
	Spartium junceum	Preti 2009, Tosi 2007	n/a	119	2.41	0.15
	Stipa tenacissima	deBaets 2008	n/a	57	23.52	3.69
	Tamarix canariensis	deBaets 2008	593	55	14.00	3.49
	Teucrium capitatum	deBaets 2008	n/a	51	12.55	1.73
	Thymelaea hirsuta	deBaets 2008	n/a	52	24.51	1.84
	Thymus serpyllum	Burlyo 2011	n/a	6	n/a	n/a
	Thymus zygis	deBaets 2008	n/a	34	10.49	3.19
Praire	Hordeum vulgarum	Loades 2010	30§	45	3.32	0.74
Tropical Evergreen	Casuarina equisetifolia	Fan 2010	809	19	n/a	n/a
	Eucalyptus camaldulensis	Abernethy & Rutherford	n/a	170	25.52	4.08
	Hibiscus tiliaceus	Fan 2010	n/a	28	30.56	3.06

	Leucaena leucocephala	Fan 2010	683	24	12.43	2.82
	Mallotus japonicus	Fan 2010	503	30	13.62	0.93
Warm Temperate Forest	*Acer rubrum*	Hales 2009	490	132	16.26	1.57
	Carya sp	Hales 2009	608	173	20.44	1.48
	Fraxinus americana	Riestenburg 1994	675	44	n/a	n/a
	Liriodendron tulipifera	Hales 2009, 2015	350	621	11.63	1.91
	Pinus palustris	Pollen 2005	540	118	16.26	0.82
	Platycladus orientalis	Ji 2012	n/a	51	12.70	1.27
	Quercus prinus	Hales 2009	570	194	23.67	1.44
	Quercus velutina	Hales 2009	715	90	10.96	1.51
	Rhododendron maximum	Hales 2009	500	378	12.80	0.70
	Robinia psuedo acacia	Burlyo 2012, Ji 2012	675	87	35.24	2.22
	Salix nigra	Pollen 2005	360	67	19.51	1.16
	Sapium sebiferum	Fan 2010	473	27	12.60	2.00
	Tsuga canadensis	Hales et al 2009	380	99	19.84	1.49

Title: Modelling biome-scale root reinforcement and slope stability

Author: Hales, T.C.*

I develop a model of root reinforcement at the biome level. The model calculates both the magnitude and range of expected root reinforcement for any biome on the planet. All biomes demonstrate high variability in root cohesion suggesting only major shifts in biome structure will cause measurable changes in landsliding.